HALF-CELL POTENTIALS AND THE CORROSION OF STEEL IN CONCRETE

Richard F. Stratfull, California Division of Highways

The half-cell potential of steel embedded in concrete specimens in laboratory tests was periodically measured and related to the visual observation of concrete cracking. It was observed that, when the half-cell potential values were more negative than -0.45 V to the saturated calomel electrode, 60 percent of the reinforced concrete blocks were cracked from the corrosion of the steel. At values between -0.27 and -0.42 V, the steel was corroding but not always enough to cause concrete cracking. In cracked concrete, the maximum half-cell potential of the steel was measured to be -0.59 V. In addition to the laboratory tests on small specimens, a prototype-simulated bridge deck was exposed outdoors to periodic wetting and drying of a chloride salt solution, and half-cell potentials were measured by using various techniques. It is shown that, once corrosion begins, the measurements will show the potential gradients of the resulting corrosion currents irrespective of the technique used to obtain them. However, there was a significant difference in the level of the potentials, and that level was clearly associated with the method of electrical measurement.

•PREVIOUS work (1-6) has demonstrated that the half-cell potential of steel in concrete is a valid indicator of corrosion activity. In effect, measurements (2, 4) of half-cell potentials have identified steel that is noncorroding (passive) when a measured value is numerically less than -0.22 V relative to the saturated calomel electrode (SCE) and corroding (active) when the value is numerically greater than -0.27 V (SCE). Between -0.22 and -0.27 V, the condition may be either active or passive.

Although an active potential of the steel does not correlate with a rate of corrosion, it is known (2, 4) that, with an increasing amount of corrosion, the numerical value of the potential also increases. Therefore, because there is concern (7) about cracking of concrete caused by rusting steel, an attempt was made to find a half-cell potential value that is indicative of the amount of steel corrosion that can cause concrete to crack and to explore some of the various techniques used to obtain half-cell potentials.

In this regard, data are given from two different tests. One test measured a single half-cell potential value for reinforced concrete that is partially immersed in a saturated solution of sodium chloride. The value in this type of test is that the half-cell potentials clearly show the noncorroding or passive state and conversely the active or corroding state of the steel.

The second test measured the half-cell potential and the potential gradients on the surface of a corroding simulated bridge deck. The half-cell potentials that are obtained on the simulated bridge deck are similar to those that would be obtained on an actual field structure. Four different techniques were used to measure the electrical potentials on the simulated bridge deck. These measurements show how the level of the measured potential can be affected by the reference electrical "ground."

Sponsored by Committee on Corrosion.

STUDY SUMMARY

The laboratory test data indicate that, when the measured half-cell potential of steel in concrete test blocks was numerically greater than -0.42 V (SCE), approximately 60 percent of 137 blocks were cracked by the rusting steel. Of the concrete blocks that were cracked by the rusting steel, the maximum measured half-cell potential was -0.59 V (SCE).

A trend in the data indicated that the measured half-cell potential of the steel that caused concrete cracking decreased as the cement factor of the concrete was increased. The variation in the potential may possibly be the result of higher electrical resistance due to an increase in the cement factor of the concrete.

The most common cement factors used in structural concrete are between 6 and 8 sacks of cement per cubic yard. The data for concrete mixes within this range indicate that a significant percentage (about 50 percent) of the concrete blocks were observed to be cracked by corrosion when the half-cell potential was numerically greater than about -0.42 V (SCE).

However, based on 95 percent of the observations of the half-cell potential of steel, the least negative potential associated with corrosion-caused concrete cracking was -0.31 V (SCE).

The results of this laboratory work indicate that a nondestructive means for measuring or detecting corrosion activity of steel can be useful for evaluating reinforcing concrete structures exposed to aggressive environments. For example, half-cell potential values that are numerically less than -0.22 V (SCE) indicate passive or noncorroding steel; for values that are numerically greater than -0.27 V (SCE) but less than -0.42 V (SCE), the steel is active but would not, on the average, be expected to have rusted enough to cause visible concrete distress except at a lower level of probability. For potential values that are numerically greater than -0.42 V (SCE), the laboratory tests showed that there is better than a 50 percent probability that good-quality concrete cover of about 1-in. thickness will have been cracked by the rusting steel, whereas concrete cracking can be expected when the potential is at least as negative as -0.31 V (SCE). However, it is important to recognize that the following must always be considered when relating concrete cracking and the half-cell potential of the steel:

1. The half-cell potential of steel can only be empirically related on a statistical basis to concrete cracking under specific conditions,
2. The half-cell potential of steel does not measure the physical or structural condition of concrete, and
3. The cracking of concrete due to the corrosion of steel is related to concrete strength, absorption, moisture content, stresses, and its thickness over the steel.

Therefore, as these latter variables change, so will the empirical relations between concrete cracking and the half-cell potential of the steel. Although it may be hazardous to use empirical relations, this laboratory work confirms that of Kliethermes (7) when he reported on the inspection of 120 exposed concrete decks from 33 states. Kliethermes found bridges to be in good condition when 90 percent of all potential readings were less negative than -0.22 V (SCE); other studies (2, 4) have shown that, in more than 99 percent of the tests, the steel was noncorroding or passive when the potential was less negative than -0.22 V (SCE). Also, Kliethermes reported that the bridge decks were in poor condition, i.e., spalled and cracked, when the potential readings were more negative than -0.32 V (SCE), whereas in this study approximately 97 percent of the cracked concrete blocks had a potential more negative than -0.32 V (SCE).

Therefore, although the empirical relation between the potentials and concrete distress can have a degree of accuracy, it must be looked on as a guide that should be tempered by more specific tests and, most important, by the judgment of the engineer. Previous laboratory work has shown (2) that, at the time of concrete cracking, the average pit depth in a ½-in.-diameter embedded steel bar that had corroded enough to cause cracking was approximately 10 mils (0.01 in.).

Because the measurements of the half-cell potential depend on an electrical circuit, variable measurements may be obtained due to the conductivity of the concrete. For example, with a surface dry concrete, the contact resistance of the half-cell to the concrete may be so great that an erroneously low potential value may be measured.

As shown by the various equipotential contours on the bridge deck test slab, care must be exercised both in obtaining the half-cell potentials and in interpreting them.

In order to evaluate the condition of a concrete structure in which all of the reinforcing may not be electrically interconnected, half-cell potentials were made on a simulated bridge deck slab where in the proper lead to the voltmeter was connected to electrically and nonelectrically connected steel. In addition, a test was made where the voltmeter was not connected to the steel but to another stationary half-cell on the surface of the concrete so as to demonstrate the feasibility of making measurements without an electrical connection to the steel.

The results of these tests show that, for all measurement techniques used in this study, the same corrosion-caused voltage gradients were measured on the concrete surface whether or not a direct electrical connection was made to the reinforcing steel. However, there was a significant difference in the level of the potentials that was clearly associated with the referenced electrical "ground."

CONCLUSIONS

In light of the foregoing, the following conclusions can be drawn:

1. Electrical potential measurements can indicate active or passive steel condition.
2. Differences in the electrical half-cell potentials are associated with the "solution potential" of the steel as well as the voltage gradients resulting from current flow.
3. In a voltage gradient, the measured half-cell may not necessarily reflect the true half-cell potential of the most proximate steel because the voltmeter can only indicate the highest voltage at that point. For example, two pieces of steel may be in close proximity to the point of measurement, one corroding and the other not corroding. The voltmeter will only indicate the highest voltage present, and thus there will be no indication of the presence of noncorroding steel.
4. To detect corrosion-caused electrical current flow, it is not always necessary to electrically connect the voltmeter to the reinforcing steel.
5. The best measure of the electrical half-cell potential is a direct electrical connection to the steel under consideration.
6. Under the condition of electrical current flow, all half-cell potential measurements will be distorted by the arithmetic difference of the associated voltage gradients.

FABRICATION OF TEST BLOCKS

The variables of concrete manufacture used in this series are given in Table 1. The river-run aggregate was $\frac{3}{4}$ in. maximum size, and the gradation complied with the 1964 standard specifications of the California Division of Highways. The cement used was ASTM Type II, modified, low-alkali, which also complied with the 1964 standard specifications.

The reinforced concrete specimens were $4\frac{1}{2}$ in. wide, $2\frac{1}{2}$ in. thick, and 15 in. long (Fig. 1). The $\frac{1}{2}$-in.-diameter steel bar was cast in the concrete to provide a nominal 1 in. of concrete cover at any point. A binding post was used to make an electrical connection from the steel bar to a recording voltmeter (Fig. 1).

Out of each batch of concrete specimens fabricated, one-half were steam-cured for approximately 16 hours at 138 ± 5 F and then post-cured in water for 28 days. All steam-cured specimens were held in their molds for a minimum of 4 hours prior to steam-curing. In all cases, the concrete was steam-cured on the day that it was mixed. The other half of the batch of specimens was cured by being completely immersed in water at a temperature of approximately 72 F for 28 days after 1 day of curing in the molds.

TESTING PROCEDURE

After the concrete curing period, the still wet specimens were partially immersed for a depth of $3\frac{1}{2}$ in. into a saturated solution of sodium chloride.

Figure 2 shows the typical testing layout for the concrete blocks. Note the multiconductor plug and cable arrangement for making electrical connections to the voltage recorder.

Electrical half-cell potentials of the steel as referenced to an SCE were made and recorded thrice weekly.

On approximately a 10-day cycle, the concrete blocks were removed from the testing tanks and visually inspected for evidence of concrete cracking. No concrete block was out of the test tank for more than 1 hour at a time.

TEST RESULTS

Figure 3 shows a typical potential record. As indicated, the half-cell potential assumes a low or passive value soon after being partly submerged in the tank and remains low until the chloride ion permeates the concrete and reaches the surface of the steel. It then causes the steel to become active. The initially high potential of the steel is caused by the film of water at the interface of the concrete where the steel projects into the atmosphere. Drying of this surface stops the active corrosion at that point, and the measurements then reflect those values for concrete-embedded steel.

The measured half-cell potential values for the 5-, 6-, and 8-sack concrete specimens are given in Tables 2, 3, and 4. The active potential values given were first measured after the salt was assumed to have reached the steel (a large jump in value). Also given are the measured potential values at the time cracking was first observed by inspection, which was usually some time later.

As shown in Figure 4, the half-cell potential of steel at the time of active potential, and the time when the concrete has been observed to have cracked, tends to numerically decrease with increasing cement factor. Also, for concrete of the same cement factor, the half-cell potentials are numerically greater in concrete that has been steam-cured. For a given cement factor there is a significant increase in the half-cell potential of the steel between the time when it is first measured to be active and the time when a crack in the concrete is first observed.

As shown in Figure 5, the average half-cell potential of the steel when it was first observed to be active was -0.36 V (SCE). The average half-cell potential of the steel in these same specimens, when cracking of the concrete was observed, was -0.47 V (SCE). Although there is a considerable overlap in the potentials, it is apparent that there is an upper range of potentials, which indicates a significant possibility of concrete cracking and significant rusting of the steel before cracking is observed. The possibility of detecting relatively large amounts of corrosion before cracking occurs is most significant.

Also, as shown in Figure 5, approximately 62 percent of the cracked concrete specimens had a potential that ranged between -0.45 and -0.59 V. Therefore, at a potential of -0.45 V or greater, rust-caused concrete cracking was observed more often than not. However, as shown in Figure 4, the half-cell potential of the steel at the time of concrete cracking, and also at the time of initial activity, significantly decreases in numerical value when the cement factor is increased from 5 to 6 sacks of cement per cubic yard. Because structural bridge concrete in California contains at least 6 sacks of cement per cubic yard, only those data for the 6- and 8-sack mixtures were used in preparing Figure 6. For 6- and 8-sack concrete, as indicated in this figure, at a half-cell potential of -0.42 V (SCE), approximately 95 percent of the first measured active potentials had a lower numerical value. At a later date when the concrete was observed to be cracked, approximately 50 percent of the rust-caused cracked concrete specimens had a half-cell potential greater than -0.42 V (SCE).

In this regard, Kliethermes (7) recently reported on the half-cell potentials and physical condition of 120 bridge decks in 33 different states. A half-cell potential of -0.42 V (SCE) is about equal to -0.50 V ($CuSO_4$) used by Kliethermes (7). He reported

Figure 1. Test specimen.

Figure 2. Partial immersion testing of steel in concrete.

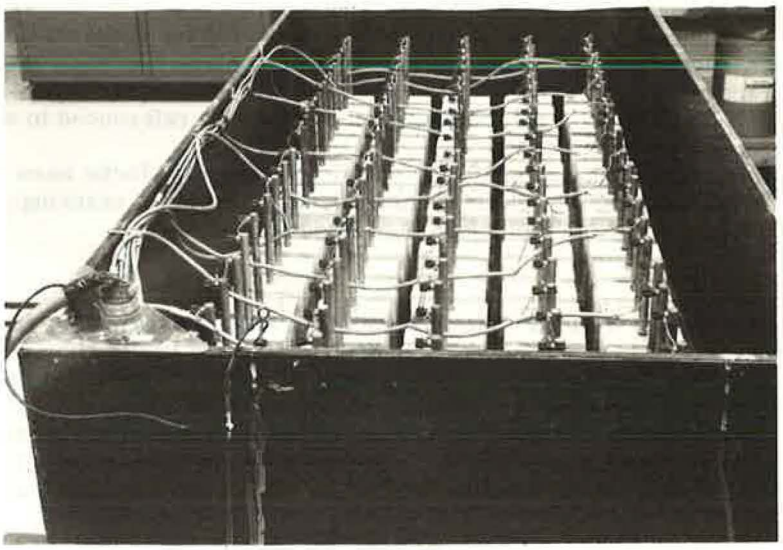

Table 1. Concrete mix variables.

Cement Factor	Nominal Slump (in.)	Air (percent)	Unit Weight (lb/ft^3)	Mixing Water (lb/ft^3)	
				Gross	Net
5.03	2¼	1.5	152.1	325	280
6.02	3¼	1.8	151.0	368	321
8.24	3½	1.6	152.5	374	331

Table 2. Half-cell potential values for 8-sack concrete specimen.

Factor	Moist-Cure		Steam-Cure	
	Active Potential (mV)	Concrete Crack Potential (mV)	Active Potential (mV)	Concrete Crack Potential (mV)
8 sacks of cement per cubic yard	290	330	360	390
	440	540	385	440
	405	305	385	470
	450	460	330	420
	305	435	340	325
	310	465	385	415
	435	425	385	485
	395	490	365	410
	315	445	340	490
	300	400	395	505
	330	320	305	385
	355	355	340	430
	—	—	315	385
	—	—	290	400
	270	360	330	540
	300	350	290	400
	365	405	295	445
	305	450	295	350
	—	—	345	515
	350	465	285	395
Potential in millivolts (SCE)	348	412	338	430
Coefficient of variation (percent)	17	17	11	13
95 percent confidence limits, $\overline{X}$ = mean	30	34	17	26

Figure 3. Typical potential record.

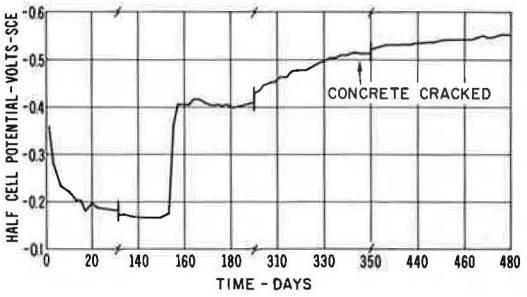

Figure 4. Cement factor and half-cell potential.

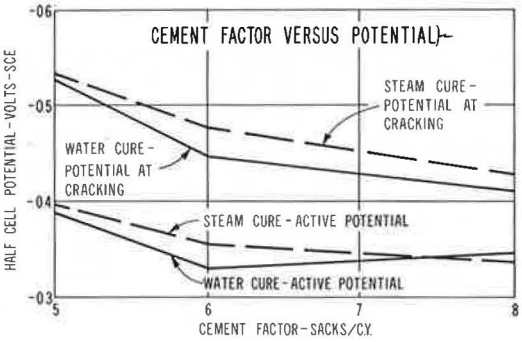

Table 3. Half-cell potential values for 6-sack concrete specimen.

Factor	Moist-Cure		Steam-Cure	
	Active Potential (mV)	Concrete Crack Potential (mV)	Active Potential (mV)	Concrete Crack Potential (mV)
6 sacks of cement per cubic yard	340	310	320	400
	350	400	340	530
	300	405	375	545
	265	460	360	560
	330	390	410	450
	375	430	360	380
	390	440	435	535
	350	345	355	435
	330	360	380	420
	375	405	400	550
	280	510	330	510
	400	500	320	530
	370	500	270	470
	295	435	340	505
	330	450	290	475
	270	345	370	390
	320	540	380	500
	360	505	320	460
	330	520	370	550
	300	530	370	400
Potential in millivolts (SCE)	333	439	355	480
Coefficient of variation (percent)	12	16	11	13
95 percent confidence limits, $\overline{X}$ = mean	18	32	19	28

Table 4. Half-cell potential values for 5-sack concrete specimen.

Factor	Moist-Cure		Steam-Cure	
	Active Potential (mV)	Concrete Crack Potential (mV)	Active Potential (mV)	Concrete Crack Potential (mV)
5 sacks of cement per cubic yard	381	569	410	533
	466	560	356	441
	472	568	416	502
	396	532	371	467
	395	510	391	548
	440	577	385	467
	455	479	401	496
	334	580	380	541
	447	585	433	501
	469	572	396	574
	390	578	340	586
	420	581	407	585
	370	579	445	524
	351	504	399	529
	419	455	419	570
	388	570	415	567
	359	557	426	588
	404	557	353	558
	419	503	476	522
	317	448	432	576
	311	501	383	536
	348	518	403	506
	344	399	428	519
	387	433	346	559
	287	477	369	481
Potential in millivolts (SCE)	391	528	399	531
Coefficient of variation (percent)	13	10	8.2	7.7
95 percent confidence limits, $\overline{X}$ = mean	21	22	14	17

that, for the 50 bridge decks that were in good condition with only minor cracking, the measured potential value of the steel did not have a numerical value greater than -0.50 V ($CuSO_4$). For 31 additional bridge decks that were rated "fair—cracked," approximately 5 percent of the decks had a measured potential that numerically exceeded -0.50 V ($CuSO_4$). For the 39 bridge decks that were rated "poor—spalled—cracked," about 50 percent of the bridges had potential values that exceeded -0.50 V ($CuSO_4$).

From this field report, it is obvious that the half-cell potential of the steel is a meaningful nondestructive technique that can be used to evaluate the condition of a reinforced concrete bridge structure with regard to active corrosion of the steel and corrosion-caused cracking of the concrete.

FABRICATION OF SIMULATED BRIDGE DECK SLAB

A reinforced concrete slab, 6 ft long and 7 ft wide, was cast containing the normal amount and position of reinforcing steel as found in bridge decks. Although two layers of steel were used, for simplicity, only the top mat of reinforcing steel is shown in Figures 7, 8, 9, and 10. The transverse reinforcing bars, No. 5's, are on 11-in. centers, and the longitudinal reinforcing steel bars, No. 4's, are on 18-in. centers. In addition, truss reinforcing bars were placed in the transverse direction on 11-in. centers. The lower mat of reinforcing steel is the same as the top mat; however, it was spaced a little off-center as normally found in bridge design.

One electrically isolated reinforcing bar is located in the top mat. The location of this one bar not touching the other steel in the mat is noted in Figure 8 by the word "ground." Also included in this test slab is a ¼-in. round by approximately 2-in. long steel probe that is embedded into the concrete with 4 in. of concrete cover. This steel probe has a wire connected to it that is brought out through the concrete to the surface to facilitate electrical measurements. The location of this probe is shown in Figure 9. It also is not connected electrically to the other embedded steel.

The concrete contained ¾-in. maximum-sized aggregate and the gradation was in accordance with the 1970 California standard specifications. The thickness of the slab is slightly less than a typical bridge deck slab, 5⅝ in. The penetration of the fresh concrete was 1¼ in., and the regular cone slump was about 2½ in. The concrete had a designed cement factor of 6 sacks of cement per cubic yard and was vibrated into place with normal vibration techniques.

The concrete cover over the top mat of steel was 1 in. After the slab was cast, it was wet-cured for 28 days. After wet-curing, it was allowed to dry for a period of approximately 6 months. A berm to hold ponded water was then constructed of wood and plastic. Thereafter, 8.6 lb (about 2 lb/yd^2) of sodium chloride were spread on top of the slab, and water was added. No further additions of salt were made and only periodic applications of water. Loss of salt during rainy weather was prevented by use of a waterproof cover.

Essentially, part of the water on the surface of the slab either evaporated into the air or was absorbed by the concrete. Once the slab surface became dry, it was reflooded with water, and cycling continued. In general, the slab would be flooded for about 1 week and dry for about 2 weeks. The first potential measurements were made prior to the first application of salt and water. Active potentials began to appear about 10 days after the salt was applied.

TESTING PROCEDURE

The slab surface was marked off at 6-in. intervals longitudinally and transversely. On this grid pattern of 6 in., center-to-center, potential measurements were made using a high-impedance voltmeter. One electrical connection was made to the SCE, which was touched to the surface of the concrete at the grid intersections. The other electrical connection to the voltmeter was made in four different ways:

1. The potential measurements were referenced to all of the reinforcing steel (Fig. 7);
2. The potential measurements were referenced to a single, long, electrically insulated reinforcing bar (Fig. 8);

Figure 5. Distribution of half-cell potentials, all concrete.

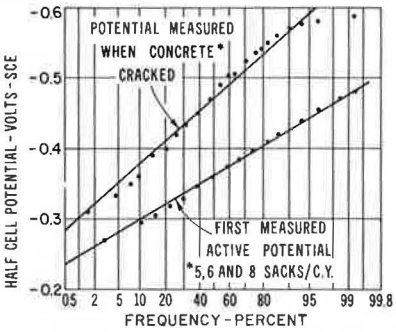

Figure 6. Distribution of half-cell potentials, 6- and 8-sack mixtures.

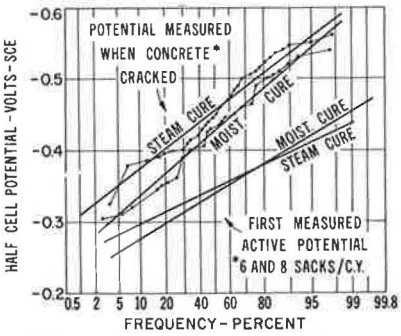

Figure 7. Equipotential contours referenced to all reinforcing steel.

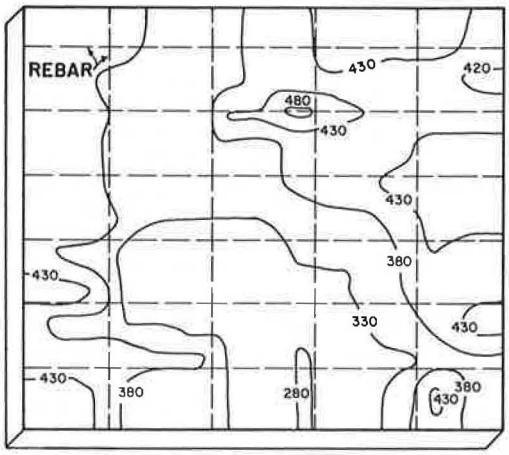

Figure 8. Equipotential contours referenced to insulated rebar.

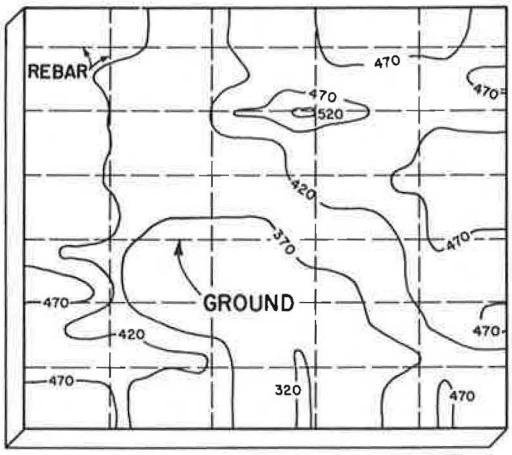

Figure 9. Equipotential contours referenced to isolated probe.

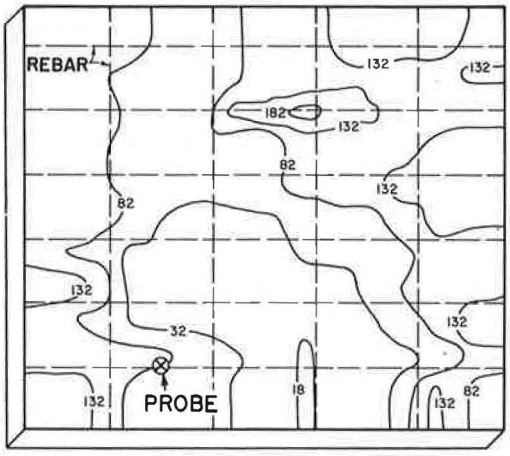

Figure 10. Equipotential contours referenced to two calomel half-cells.

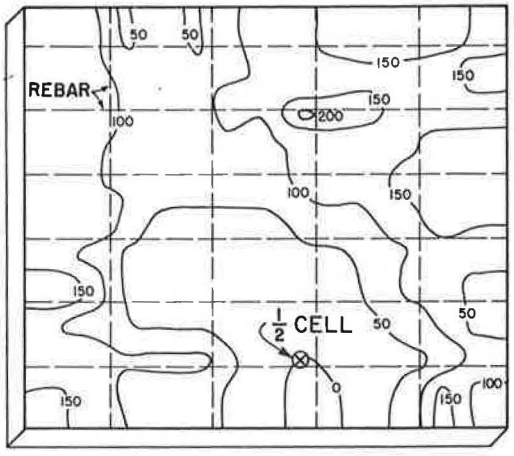

3. The potential measurements were referenced to an electrically isolated steel probe that is embedded 4 in. down in the concrete (Fig. 9); and
4. The potential measurements were referenced to an SCE that was left in place on top of the slab (Fig. 10).

Using voltage readings from each series of measurements, equipotential contours were drawn at 50-mV intervals.

TEST RESULTS

Figures 7, 8, 9, and 10 are equipotential contour maps for the simulated bridge deck obtained by using the four different methods of measurements described.

For simplicity, the word "ground" is used to denote the location of one electrical connection. However, the equipotential contours shown in Figures 7, 8, 9, and 10 are actually referenced to the electrical connection of the reinforcing mat, the rebar, etc. Therefore, it will be noted on the four figures that the level of the potential contours varies in accordance to the technique for making the measurements, but the general location of the contour lines is the same for each method of measurement.

Figure 7 shows the contour intervals when the half-cell was referenced to embedded reinforcing steel mats. As shown by the contour intervals, there are variations of the half-cell potentials of the steel caused by the corrosion of the steel and the associated flow of electrical current.

In Figure 8, the half-cell potentials were obtained by grounding the voltmeter or referencing the half-cell to a single, long, electrically isolated piece of reinforcing steel in the concrete. As will be noted, there is a great similarity between potential contours that were obtained even though two methods for grounding were used.

The contours shown in Figure 9 were obtained from measurements made when one terminal of the voltmeter was connected or grounded to the small, electrically insulated probe embedded in the slab. The equipotential contours were then drawn using this probe as a reference for the measurements. It will be noted that again there is a great similarity among the equipotential contours obtained by the three methods of grounding as shown in Figures 7, 8, and 9.

In order to clearly demonstrate the feasibility of obtaining potential measurements without an electrical connection to the steel, two SCE's appropriately connected were used to obtain electrical potential measurements. If there were no corrosion-caused current flow in the concrete, the measured voltage between these two half-cells would always be essentially zero irrespective of where either half-cell was placed on the concrete. The location of the stationary half-cell is shown by the arrow in Figure 10. This half-cell was left in place and never moved during the entire period of the measurements. The other half-cell was moved about to the 6-in. grid locations. The measurements were then used to draw the contours shown in Figure 10. As will be noted, the contours are similar in Figures 7, 8, and 9. Although the contours are similar, the potential values are not. Therefore, it is obvious that care must be exercised in making electrical connections to determine the true value of the electrical potential of the steel. This is particularly true if the measurements are to be used as an indicator of the presence of active or passive corrosion conditions.

The general procedures and techniques described can be adapted to field survey methods (7). Grid spacing is increased to keep the number of measurements to a practical level, but smaller spacing is necessary to delineate small active areas.

ACKNOWLEDGMENTS

The author wishes to acknowledge the work and other contributions of the staff at the California Division of Highways, including C. R. Lesan, C. G. Yeaw, G. C. Chang, P. J. Jurach, Faye Penrose, Betty Stoker, Marian Ivestor, Dale Drinning, D. L. Spellman, and John L. Beaton.

The contents of this report reflect the views of the author, who is responsible for the facts and the accuracy of the data presented herein. The contents do not necessarily reflect the official views or policies of the State of California or the Federal Highway Administration. This report does not constitute a standard, specification, or regulation.